Small Sample Image Recognition Based on CNN and RBFNN

Biyuan Yao[1], Hui Zhou[2], Jianhua Yin[3], Guiqing Li[1], Chengcai Lv[4]

[1] School of Computer Science and Engineering, South China University of Technology, China
[2] School of Computer Science and Cyberspace Security, Hainan University, China
[3] School of Science, Hainan University, China
[4] Institute of Deep-sea Science and Engineering, Chinese Academy of Sciences, China
yaobiyuanyy@163.com, zhouhui@hainanu.edu.cn, yinjh@hainu.edu.cn, ligq@scut.edu.cn, lvchengcai@idsse.ac.cn

Abstract

Identification of dangerous goods based on images plays a key role in the security inspection of various situations such as airports, subways, public places etc. This paper discusses the issue in a from-simple-to-complex manner. Firstly, we classify different kinds of knives given an image including a single object without complex background in the framework of TensorFlow. Then, according to the color and shape features of a single image, where Fourier transform and Roberts operator is used to judge of the complex scene which doesn't contain knives from an image with natural background. Finally, convolution neural network (CNN) and radial basis function neural network (RBFNN) are used to construct identification models for images of objects in six categories. The obtained accuracy of the true and predicted values of the CNN and RBFNN are 66.67% for training on CNN and 76.67% on RBFNN, for testing 50% on CNN and 44.44% on RBFNN respectively. The results showed that the constructed of identification model is able to perform recognition for small-scale image database and reduce the false alarm rate. Furthermore, our method is robust in dealing with the small sample, with high classification accuracy and low cost. The models have few layers and nodes.

Keywords: Image recognition, TensorFlow, Fourier transform, Roberts operator, CNN, RBFNN

1 Introduction

In recent years, various contradictions are becoming increasingly prominent in society. Government authorities and security agencies have been regularly encountered violent crimes and illegal acts, resulting in a significant loss of personal and property safety of the state. So, it's necessary to identify attention on the detection of dangerous goods. Image recognition [1-2] refers to technologies that establish a model for the information contained in input images. This is achieved through the analysis and extraction of image features, which are then used to establish a classifier to recognize the targets of different patterns according to the image features analysis. Deep learning (DL) transforms a large amount of training data into a higher level with more abstract features through simple nonlinear models [3-5]. Figure 1 shows that the field of DL experienced two troughs before its rise in 2006, which divided the development of neural network into three different stages.

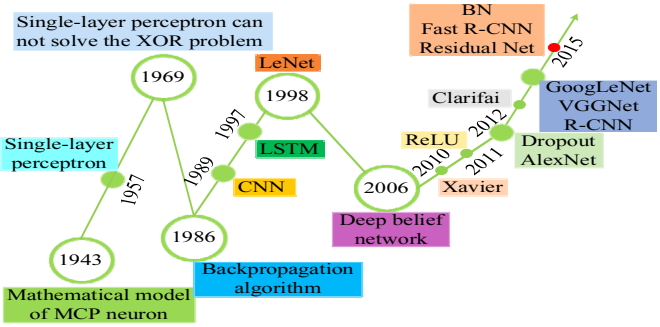

Figure 1. Development process and key nodes of DL

In research view of the shortcomings of dangerous goods image detection methods, different sample angles increase the difficulty of resolution. The color and shape characteristics of the sample image constitute the uncertainty of detection. Based on this, image recognition of dangerous goods with single high frequency is carried out, which innovatively solves the key problems in image recognition of small samples of dangerous goods based on CNN and RBFNN. In our research, main innovations are as follows: (i) in the framework of TensorFlow, given an image, the category of the target image and its recognition rate are obtained. And (ii) the recognition model of the image is proposed to continuously improve the dangerous goods sample database from small to large based on CNN and RBFNN. The database is collected from the safety inspection in Sanya city station in Hainan province, PRC (People's Republic of China) as the test sample.

*Corresponding Author: Hui Zhou; E-mail: zhouhui@hainanu.edu.cn
DOI: 10.3966/160792642020052103025

The rest of this paper organize as follows, Figure 2 is the organization chart. Section 2 describes related work and predecessors in the field of image recognition. Section 3 describes the theoretical foundation. Section 4 describes the analysis of visual feature of the image, and section 5 describes experimental verification is constructed to complete recognition of the images based on CNN and RBFNN. Finally, section 6 concludes the paper with limitation and future direction.

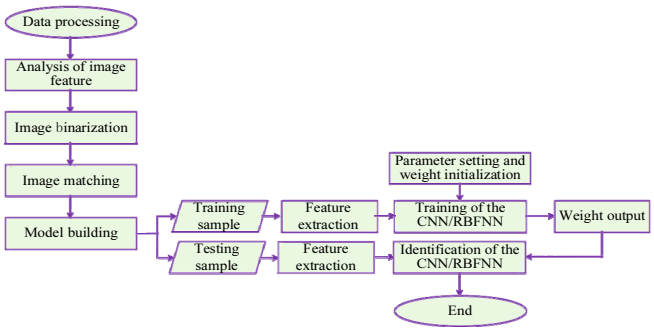

Figure 2. Organization chart

2 Related Works

Domestic and foreign scholars have carried out extensive and in-depth work in this field. Mery et al. [6] introduced a novel method on deep learning to find harmful objects in X-ray images. It's trained AlexNet [7] and GoogleNet [8] to extract the depth of features of X-ray images, using the nearest neighbor classifier (KNN) to distinguish harmful items, thereby avoiding over-fitting owing to the shortcomings of training sets. Bolei Zhou et al. [9] used proposed a method for scene classification based on CNN, which chose three popular CNN architectures, AlexNet, GoogLeNet, and VGG 16 convolutional-layer for CNN. Then they trained them on Places205 and Places365-Standard respectively to create baseline CNN models. Samet Akcay et al. [10] introduced a technique for the classification of X-ray baggage images using state of the art convolutional neural networks. It's based on the shapes of 300 groups of harmful goods images. The researchers in [11] used the one-to-one algorithm for multi-classification using a support vector machine (SVM). Which was implemented to train and recognize the extracted features, and the recognition rate was reached 93%.

3 Method

3.1 Image Processing

Image binarization means that only the black and white binary values are retained in the whole image. Each pixel takes two discrete numerical value (0 or 1), where 0 is black and 1 is white [12-14]. In the process of collecting the items, the image of the collected items may be tilted to some extent due to various reasons. Therefore, it's necessary to tilt the image correction facilitating the subsequent detection and identification. Assuming that, the point (x_0, y_0) rotates θ degrees after the point (a, b), and the coordinate is (x_1, y_1), and the center coordinates after rotation is (c, d).

$$\begin{bmatrix} x_1 \\ y_1 \\ 1 \end{bmatrix} = \begin{bmatrix} 1 & 0 & c \\ 0 & -1 & d \\ 0 & 0 & 1 \end{bmatrix} \begin{bmatrix} \cos\theta & \sin\theta & 0 \\ -\sin\theta & \cos\theta & 0 \\ 0 & 0 & 1 \end{bmatrix} \begin{bmatrix} 1 & 0 & -a \\ 0 & -1 & b \\ 0 & 0 & 1 \end{bmatrix} \begin{bmatrix} x_0 \\ y_0 \\ 1 \end{bmatrix} \quad (1)$$

Edge refers to the place where the information of depth or structure mutated, which is the end of one area and the beginning of another [15]. The operator proposed by Roberts is an operator using the local differential operator to find the edge. For the image $f(x, y)$, the edge of detection operator is to approximate the gradient operator with the vertical and horizontal difference of the image [16]. It is defined as:

$$\nabla f = (f(x, y) - f(x-1, y), f(x, y) - f(x, y-1)) \quad (2)$$

Among them, (x, y) represents the position of the image, ∇f points out the fastest direction and number of gray changes. The formula for the Roberts operator is:

$$R(i,j) = \sqrt{[f(i,j) - f(i+1, j+1)]^2 + [f(i, j+1) - f(i+1, j)]^2} \quad (3)$$

Where $f(i, j)$ and $g(i, j)$ are the gray values of the points (i, j) before and after processing, respectively. The corresponding template of Roberts operator is as follows:

$$\begin{bmatrix} 1 & 0 \\ 0 & -1 \end{bmatrix} \begin{bmatrix} 0 & 1 \\ -1 & 0 \end{bmatrix} \quad (4)$$

3.2 Fourier Transform

Fourier transform is the conversion of an image from a spatial domain to a frequency domain. Let the discrete function $f(x, y)$ represent a digital image of size $M \times N$, where $x=0,1,\ldots, M-1$; $y=0, 1, \ldots, N-1$, the two-dimensional discrete Fourier transformation $f(x, y)$ represented by $F(u, v)$ is given by the following formula [17]:

$$F(u,v) = \sum_{x=0}^{M-1} \sum_{y=0}^{N-1} f(x,y) e^{-j2\pi\left(\frac{ux}{M} + \frac{vy}{N}\right)} \quad (5)$$

Among them, $u=0, 1,\ldots, M-1$; $v=0, 1,\ldots, N-1$.

3.3 Convolution Neural Network

CNN is a feed-forward neural network (FFNN), which consists of three parts [18-19] such as: convolution layer, pooling layer and fully connected layer. Convolution operation mainly aims at two-dimensional images, and the weight of a set of $k \times k$ window size is used to carry out the related operation with each $k \times k$ small block in the input graph. Then, the value of a single atom in the output feature graph is obtained through the activation of the nonlinear function. Finally, weight sharing and sliding the window mechanism is used to iterate through the input image in the same set to obtain a two-dimensional output feature map. Each output feature graph is a linear combination of the convolution result of the multiple of input feature graphs [20]. The specific expression shows as follows:

$$x_j^{out} = f(\sum_{i \in M_j} x_i^{in} * k_{ij}^l + b_j^l) \quad (6)$$

Among them, M_j represents the set of input characteristic maps. * represents the convolution operation. x_i^{in} is the input of i, x_j^{out} is the output characteristic graph of j, k_{ij}^l is the convolution kernel matrix, b_j^l is the bias matrix, and f expresses the nonlinear mapping function. The pooling operation is mainly used for the sampling operation of the feature graph, which can be expressed as:

$$x_j^{out} = f(down(x_i^{in})) \quad (7)$$

Among them, down (•) represents the pooling function. The full connected layer feature vector x^{out} of the output layer can be expressed as follows [21]:

$$x^{out} = f(w^{out} x^{in} + b^{out}) \quad (8)$$

Among them, w^{out} is a weight matrix, b^{out} is a bias vector, and f is a non-linear mapping function.

3.4 Radial Basis Function Neural Network

RBFNN is a kind of pre-direction network with good performance, which widely used in the field of image processing. Figure 3 shows that the RBFNN of n-h-m structures, and the network has n inputs, h hidden nodes, and m outputs. Among them, $x=(x_1, x_2,\ldots, x_n)^T \in R_n$ is the network input vector, $W \in R^{h \times m}$ is the output weight matrix, $b_0,\ldots, b_m$ is offset for the output unit, $y=(y_1, y_2,\ldots, y_n)^T$ is the output of network, $\Phi_i(*)$ is the activation function of the i-th implicit node. In Figure 3, output node Σ indicates that the neurons of the output layer adopt the linear activation function. C_i represents center value of the i-th implicit node of the data in the network. ||*|| represents the European norm. The k-th output of RBFNN can be expressed as follows:

$$y_k = \sum_{i=1}^{h} \omega_i \Phi_i(\| x - C_i \|) \quad (9)$$

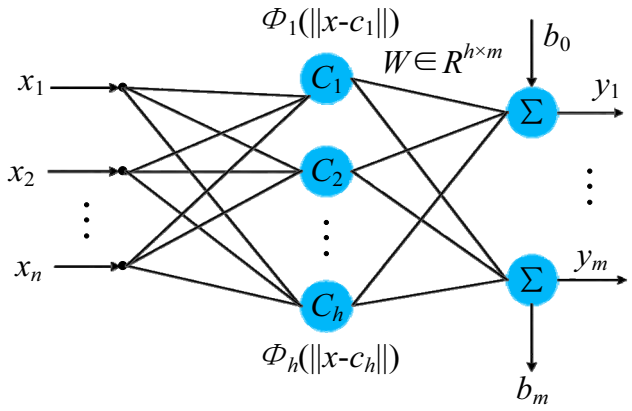

Figure 3. The structure of RBFNN

4 Visual Features of Images

Overview. Given Figure 4, the target category is given and its recognition rate is calculated under the TensorFlow framework.

Figure 4. Knife

As can be seen from Figure 5, the recognition rate of the dagger sheath is 0.47929. The carver, meat cleaver and axe have a recognition rate of 0.3396. The recognition rate of letter opener, paper cutter and scudding knife is 0.04095. Next, two-dimensional discrete Fourier transform is carried out on the image. According to the color features and shape features of the image, objects are detected and judged in the complex scene to recognize harmful items, like as knives.

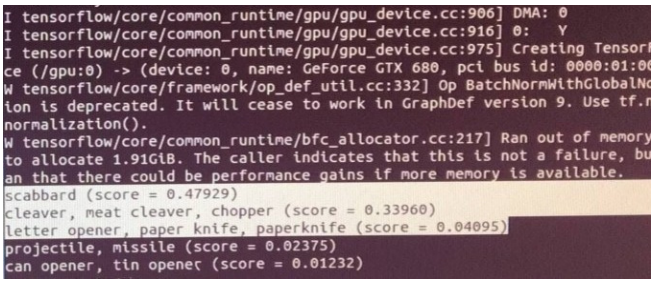

Figure 5. Results of TensorFlow identification

4.1 Color Characteristics to Image Recognition

Overview. Color characteristics have good invariance and robustness compared with other visual features which are easy to calculate. Therefore, the description

of complex scenes according to the color features is shown in Figure 6(b), which doesn't contain knife-type dangerous goods in Figure 6(a).

Figure 6(c), Figure 6(d) and Figure 6€ are obtained through the two-dimensional Fourier transform of the image. This transform the spatial representation of an image into a frequency representation. The high frequency part of the image contains the largest amount of information, and appears in the spatial domain as an inflection point, angle or a discontinuity. Here, the edges and texture regions of the image change quickly. The flat part of the region indicates that the image changes slowly and at a low frequency. Figure 6(c) has only the spectrum peak, which has a maximum value of 1.93×10^6, and indicating that there is only one dangerous item in the image. Figure 6(d) shows that the peaks of the objects in a complex scene are different, and indicating a variety of objects which is the height of the spectral peaks of similar items. Figure 6(e) shows the peak height of the spectrum, which has only one in the highest peak (a value of 3273) and a large gap between the peak values of the dangerous goods. It can be seen that dangerous goods like knives are not included in the article.

(a) Knife

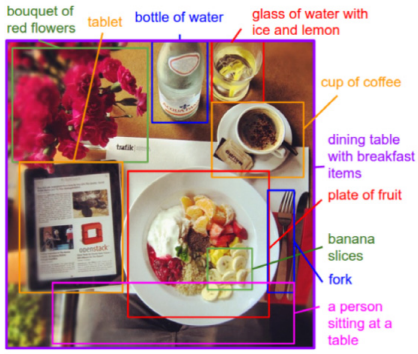

(b) Complex scene

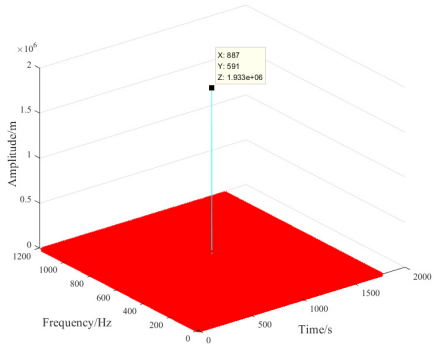

(c) Peaks of knife

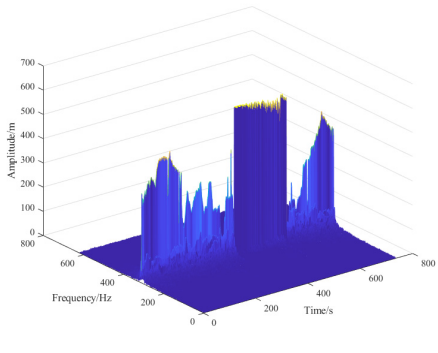

(d) Peaks of complex scene item

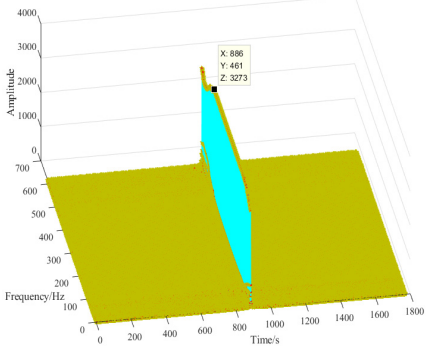

(e) Relevance of knife and complex scene

Figure 6. Color features detection of objects

4.2 Shape Features to Image Recognition

Shape features do not change in the surrounding environment, and provide the stable information for the object. Therefore, the contour-based Roberts operator is used to describe the contours of the target area surrounded. The target area surrounded is displayed by Figure 7(a) and Figure 7(b), to indicate the complex scene by Figure 7(b), where Figure 7(a) doesn't contain the harmful object in knife.

Figure 7(a) and Figure 7(b) extract the edges of the image, which contain useful information for recognition and provide an important feature parameter. In Figure 7(c), Figure 7(d) and Figure 7(e) describe the flat region of the most image constituting of the content of the image, there are many components in low frequency. The origin of the coordinate system is moved to the center of the image. The center is the low frequency and the periphery is the high frequency. Figure 7(c) and Figure 7(d) are the horizontal section of the maximum values of the image. Figure 7(e) shows the spectrum image of the dangerous items and the complex scene has only one maximum peak of 5.06, and not two peaks. Therefore, the dangerous item (the knife) does not exist in the image of the complex scene.

(a) Knife

(b) Complex scene

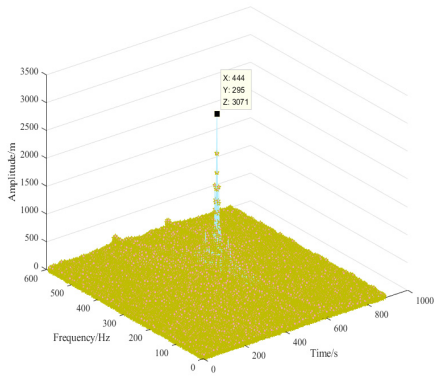

(c) Peaks of knife

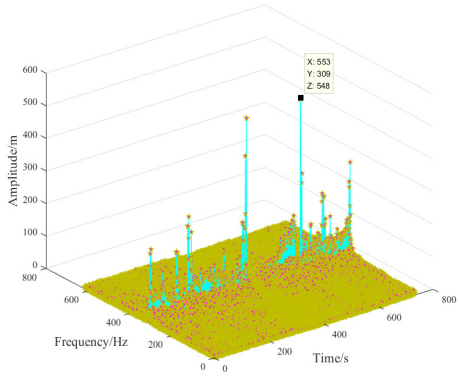

(d) Peaks of complex scene item

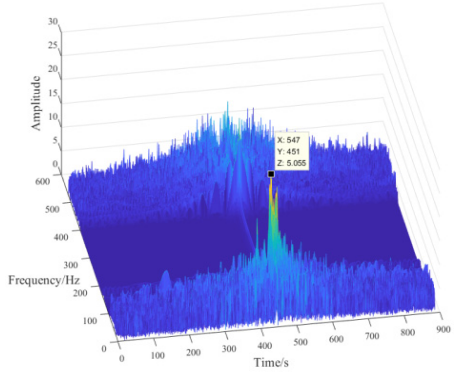

(e) Relevance of knife and complex scene

Figure 7. Shape features detection of objects

5 Experimental Verification

Overview. The data is divided into training and testing samples. CNN and RBFNN are used to identify small samples of dangerous goods, and accuracy.

5.1 Identification Model of CNN

Neural network training is carried out for the given samples, and the network structure is determined. By the mentioned step's recognition task is performed as follows.

5.1.1 Experimental Data

The data has 120 training samples, including axes, knives, lighters, scissors, objects sharp and suspicious, and objects ordinary harmless. The image of each item contains five different images of the same type with five different styles (such as differences in shape, color, background and so on). Each image is divided by rotating at four angles in order to reduce the negative influence of angles, and forms part of the sample data sets (see Figure 8). At the same time, considering that images of metal are blue in general, the training samples are taken as non-blue, so there are 120 training samples to be input. In the sample output, "1", "0" and "-1" represent must contain, may contain, and do not contain dangerous samples (see Table 1), respectively.

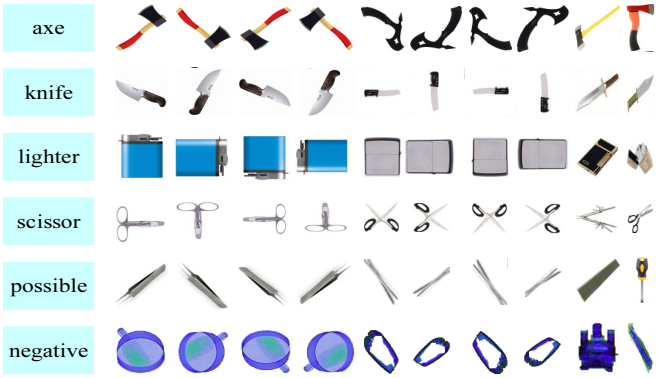

Figure 8. Six types of training samples

Table 1. Training sample mark

input	output	output mark
axe	5	1
knife	4	1
lighter	3	1
scissor	2	1
possible	1	0
negative	0	-1

In Table 1, the output for axe, knife, lighter, and scissor is "5", "4", "3" and "2" respectively. They are high-dimensional dangerous goods. Their output of marks is recorded as "1", indicating that the sample

must contain dangerous samples. If the "possible" output is "1", then it is suspicious and possibly dangerous goods. If the "possible" output mark is "0", then this indicates that it may contain dangerous samples. If the "negative" output is "0" then they are harmless goods. If the "negative" output mark is "-1" then this indicates that it does not contain dangerous samples.

There are 18 test samples in the dataset, and the images from each test sample are different with respect to shape, color, background and so on.

5.1.2 Analysis of Experimental Results

The input layer image size is set to 300×300, and there are five convolutional layers (convolutional kernels of size is 5×5, and three layers of 4×4). The down-pooling is of size five (i.e. five layers of 2×2). There are 120 training samples.

Figure 9 reduces the number of parameters through local perception. Each local receptive field is mapped to a neuron in the convolutional layer through a convolution kernel. The figure shows an image of size 300×300. The receptive field size is 5×5 and the length of the moving step is 1, then the number of eventual receptive field is: $(1500\text{-}5+1)^2=14962$, which is 2.2×10^6. Figure 9(a) is the full connection, with a total weight of 8.1×10^9. Figure 9(b) is a local connection, with a total weight of 2.25×10^6.

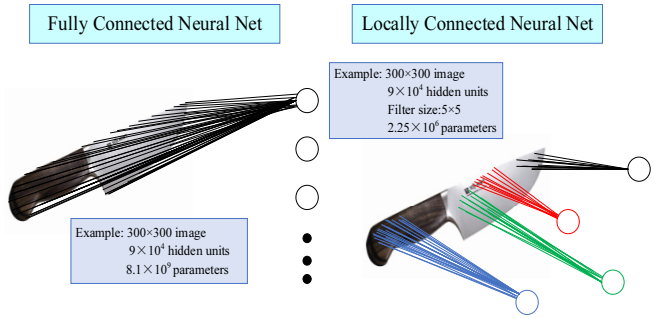

(a) (b)

Figure 9. Full connection (BP network) and local connection (convolution network)

Figure 10(a) shows the error curve after judgment. The error between the real value and the test value is zero, which means that the judgment is correct. With increasing testing samples, the error fluctuates between 0%-2% and the error fluctuation amplitude tends to be stable. Figure 10(b) is an analysis of the real value and predicts value of the training samples. The accuracy is 66.67%. Blue dots express the predicted value and the red dots express the true value. When the predicted value (blue dots) coincides with the true value (red dots), the accuracy of the simulation test is 100%. Next, a test model is performed on the image, as shown in Figure11.

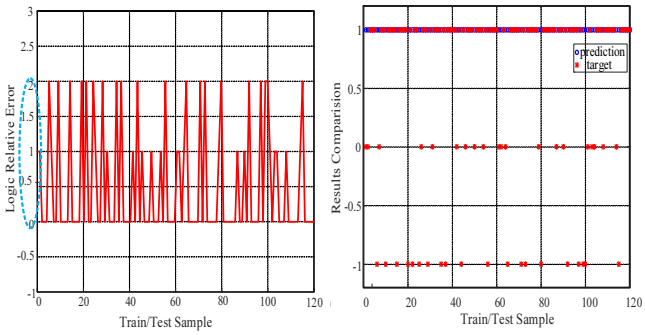

(a) (b)

Figure 10. Simulation training data

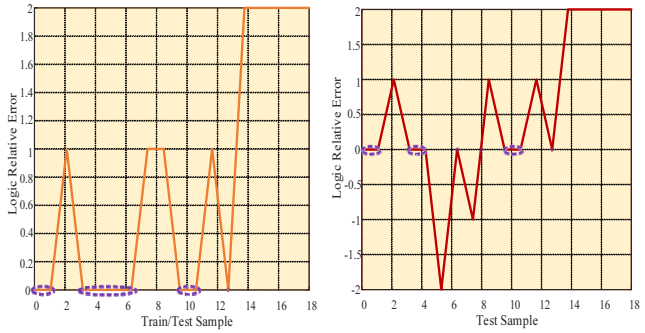

(a) (b)

Figure 11. The effectiveness of test model

Figure 11(a) is the real output of the error curve. Some samples are not output because the outputs of the real value are zero and are used as the denominator. Figure 11(b) is an analysis of the actual value and predicts value of the test samples. The accuracy rate is 50%. The effectiveness of the algorithm is verified by simulation experiments with test samples.

5.2 Identification Model of RBFNN

The image database is divided into learning stage and the classification stage. RBFNN is used to modify the relevant parameters to identify the image, improve the classification accuracy and speed.

5.2.1 Experimental Setup: Generate Training Samples and Test Samples

The image data is divided into training samples and testing samples.

5.2.2 Analysis of Experimental Results

The neural network toolbox provides a variety of supervised learning models, self-organizing graphs and unsupervised learning models with competitive layers [22]. Therefore, using the toolbox for the radial basis function neural network, training is performed by inputting sample data. The RBFNN identification model is constructed (see Figure 12).

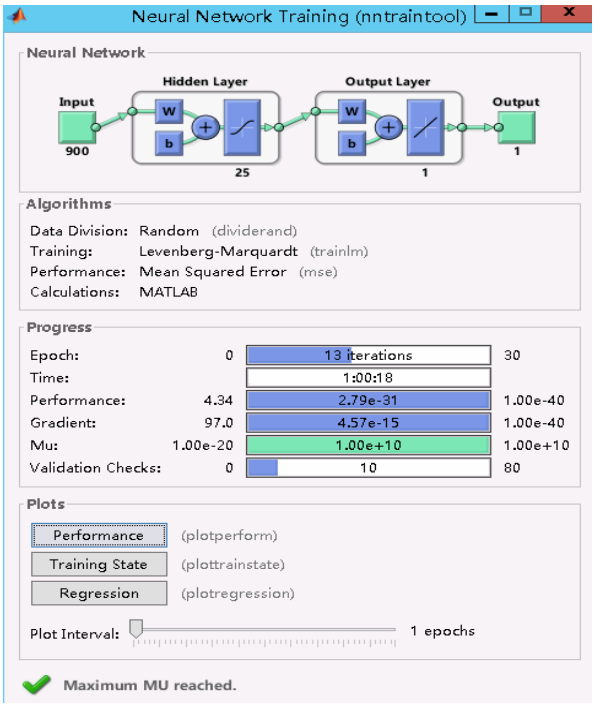

Figure 12. Execute interface

Figure 13 shows that the input layer of the RBFNN has 900 neurons, and 1 neuron in the output layer. In general, if the problem is more complex, the more neurons need to be set, with more layers of neurons. Here, there are 25 neurons in the hidden layer. Training is 30 steps, and its running time is 1 hour. The RBFNN simulation test is performed using the image data (see Figure 13). Figure 13(a) shows the error curve of the real output. Figure 13(b) shows the error curve after judgment. The error is zero, which means that the judgment is correct. Figure 13(c) is an analysis of the real value and predicted value of the training samples, and the accuracy of the training sample is 76.67%. The effect diagram obtained after RBFNN test of image data is shown in Figure 14. Figure 14(a) shows the error curve of the real output. Some samples are not output because the outputs of the real value are zero and used as the denominator. Figure 14(b) illustrates the error curve after judgment where the error is zero, which means that the judgment is correct. Figure 14(c) shows an analysis of the real value and predicted value of the testing samples, and the accuracy is 44.44%.

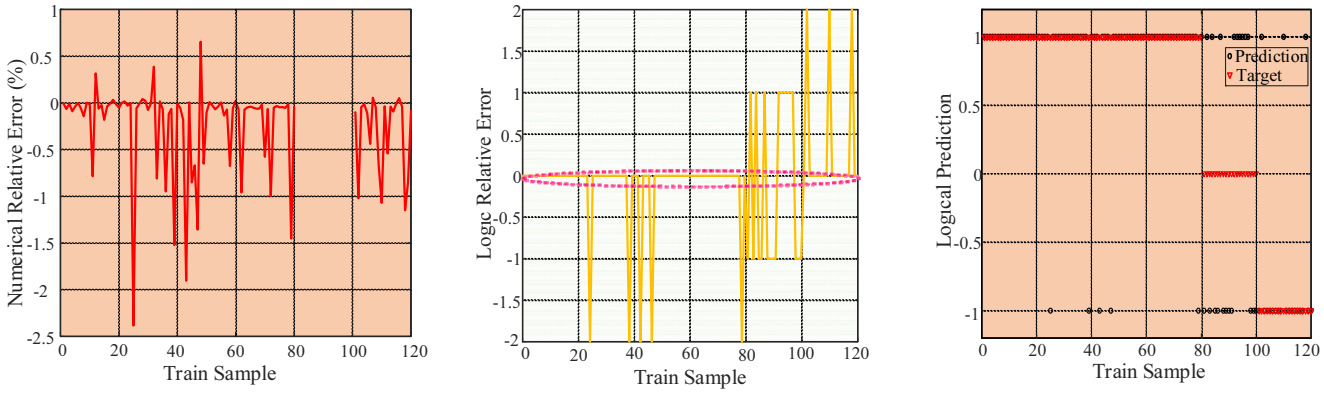

(a) (b) (c)

Figure 13. Simulation training data

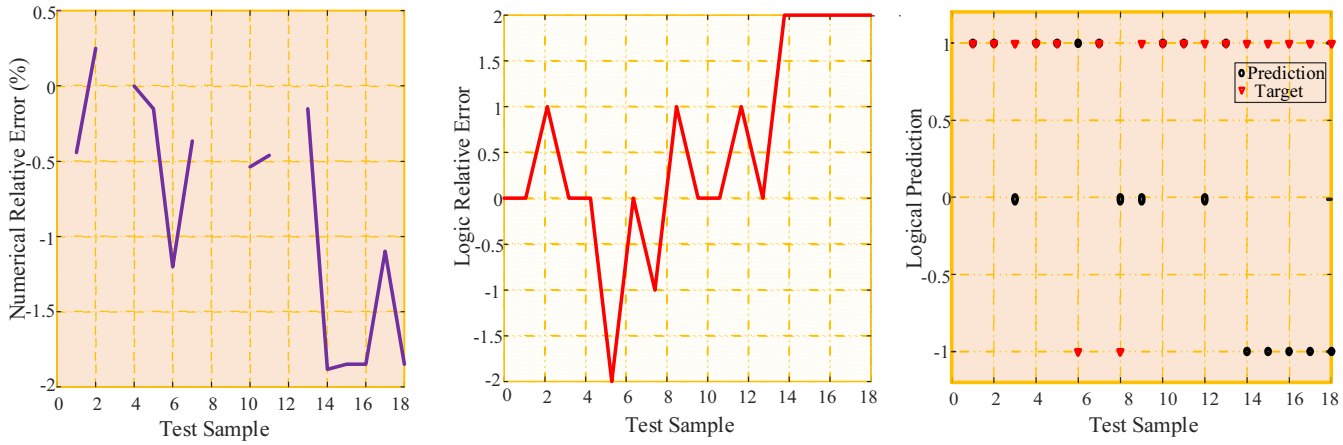

(a) (b) (c)

Figure 14. Effectiveness of test model

6 Conclusion

Table 2 shows that CNN is the better network topology than RBFNN in image processing, but RBFNN should further simplify the network and shorten the time of network training. The limitation of the study is that the images of dangerous objects are background-free and single-item. This over-idealized sample is inconsistent with the large number of images with complex backgrounds, multiple objects and mutual occlusion in the real scene. The number of samples affects the recognition rate. If the number of experiments used small number of samples, the identification error is increased significantly. In the future work, we will improve the sample database of dangerous goods from small to large, and establish the recognition of dangerous goods images in the multiple of complex scenarios, so far reduce the false alarm rate. At the same time, image recognition technology is optimized to improve the accuracy of image recognition.

Table 2. Image Recognition by the CNN and RBFNN

		CNN	RBFNN
Training sample	Recognition rate	66.67%	76.67%
	Error curve	As the increasing of testing sample, the error judgment fluctuates within 0%~2% and the error fluctuation amplitude tends to be stable.	When the fluctuation amplitude error curve is slow, and the judgment is correct.
Testing sample	Recognition rate	50%	44.44%
	Error curve	When the error is zero, and the judgment is correct.	When the error is zero, and the judgment is correct.

Acknowledgements

This work is supported by National Natural Science Foundation of China (Grant No. 61662019). Natural Science Foundation of Hainan Province (No. 117212). Nature Science Foundation of Guangdong Province (No. 2017A030313347).

References

[1] X. Wang, X. Wang, *OpenCV + VTK + Visual Studio Image Recognition Application Development*, Posts & Telecom Press, 2019.

[2] Q. Cui, Z. Zhou, C. Yuan, X. Sun, Q. M. J. Wu, Fast American Sign Language Image Recognition Using CNNs with Fine-tuning, *Journal of Internet Technology*, Vol. 19, No. 7, pp. 2207-2214, December, 2018.

[3] Y. LeCun, Y. Bengio, G. Hinton, Deep Learning, *Nature*, Vol. 521, No. 7553, pp. 436-444, May, 2015.

[4] J. Li, J. Li, Prompt Image Search with Deep Convolutional Neural Network Via Efficient Hashing Code and Addictive Latent Semantic Layer, *Journal of Internet Technology*, Vol. 19, No. 3, pp. 949-957, May, 2018.

[5] Y. Li, J. Li, J.-S. Pan, Hyperspectral Image Recognition Using SVM Combined Deep Learning, *Journal of Internet Technology*, Vol. 20, No. 3, pp. 851-859, May, 2019.

[6] D. Mery, E. Svec, M. Arias, V. Riffo, J. M. Saavedra, S. Banerje, Modern Computer Vision Techniques for X-Ray Testing in Baggage Inspection, *IEEE Transactions on Systems, Man, and Cybernetics: Systems*, Vol. 47, No. 4, pp. 682-692, April, 2017.

[7] A. Krizhevsky, I. Sutskever, G. E. Hinton, ImageNet Classification with Deep Convolutional Neural Networks, *Twenty-sixth Conference on Neural Information Processing Systems (NeurIPS)*, Lake Tahoe, California, 2012, pp. 1097-1105.

[8] C. Szegedy, W. Liu, Y. Jia, P. Sermanet, S. Reed, D. Anguelov, D. Erhan, V. Vanhoucke, A. Rabinovich, Going Deeper with Convolutions, *IEEE 2015 Conference on Computer Vision and Pattern Recognition (CVPR)*, Boston, Massachusetts, 2015, pp. 1-9.

[9] B. Zhou, A. Lapedriza, A. Khosla, A. Oliva, A. Torralba, Places: A 10 Million Image Database for Scene Recognition, *IEEE Transactions on Pattern Analysis and Machine Intelligence*, Vol. 40, No. 6, pp. 1452-1464, June, 2018.

[10] S. Akcay, M. E. Kundegorski, M. Devereux, T. P. Breckon, Transfer Learning Using Convolutional Neural Networks for Object Classification within X-ray Baggage Security Imagery, *The 23th IEEE International Conference on Image Processing (ICIP)*, Phoenix, Arizona, 2016, pp. 1057-1061.

[11] D. Ling, *Research on Image Recognition Algorithm for Millimeter Wave Hidden Dangerous Goods Imaging*, Master Thesis, Harbin University of Technology, Shenzhen, China, 2017.

[12] Y. Liu, F. Zhan, *MATLAB Image and Video Processing Practical Examples*, Publishing House of Electronics Industry, 2015.

[13] Y. Liu, S. N. Srihari, Document Image Binarization Based on Texture Features, *IEEE Transactions on Pattern Analysis and Machine Intelligence*, Vol. 19, No. 5, pp. 540-544, May, 1997.

[14] Y. Chen, L. Wang, Broken and Degraded Document Images Binarization, *Neurocomputing*, Vol. 237, pp. 272-280, May, 2017.

[15] Y. Du, *Research on Edge Detection Algorithm of Deep Image Based on Genetic Neural Network*, Master Thesis, Harbin

University of Science and Technology, Harbin, China, 2009.
[16] D. Yang, H. Zhao, Z. Long, *Detailed Explanation of MATLAB Image Processing*, Tsinghua University Press, 2013.
[17] R. C. Gonzalez, R. E. Woods, S. L. Eddins, *MATLAB Implementation of Digital Image Processing*, Tsinghua University Press, 2013.
[18] X. Feng, *Research of Image Recognition Algorithm Based on Depth Learning*, Master Thesis, Taiyuan University of Technology, Taiyuan, China, 2015.
[19] D. Mishkin, N. Sergievskiy, J. Matas, Systematic Evaluation of Convolution Neural Network Advances on the Imagenet, *Computer Vision and Image Understanding*, Vol. 161, pp. 11-19, August, 2017.
[20] S. Ashutosh, S. A. Roy, D. S. Madhurima, Creating Convolutional Neural Network and Training it to Classify Images using Machine Learning, *Indian Journal of Public Health Research & Development*, Vol. 10, No. 5, pp. 839-844, May, 2019.
[21] H. J. I. Goodfellow, Y. Bengio, A. Courville, *Deep Learning*, Posts & Telecom Press, 2017.
[22] S. Yu, *Case Analysis and Application of MATLAB Optimization Algorithm*, Tsinghua University Press, 2014.

Biographies

Biyuan Yao is currently pursuing her Ph.D. degree in School of Computer Science and Engineering, South China University of Technology, China. Her research interests include image processing, computer graphics and graph theory with applications.

Hui Zhou received B.S. degree from University of Science and Technology of China (USTC), and Ph.D. degree from University of Chinese Academy of Science. Dr. Zhou has worked in IBM China Research Laboratory for several years, and has been an associate professor of Hainan University since 2011. Dr. Zhou is in charge of several research projects including the National Natural Science Funds projects. His research interests include writing robot, data visualization, cluster file system.

Jianhua Yin is Professor of Hainan University, MS supervisor. His research interests include graph theory with applications.

Guiqing Li works at the School of Computer Science and Engineering, South China University of Technology, China. His research interests focus on fields related to Computer Graphics such as digital geometry processing, dynamic geometry processing, and image and video processing.

Chengcai Lv received the B.S. degree, M.S. degree from Harbin Engineering University, PRC, in 2011 and 2014. He is working in the Institute of Deep-sea Science and Engineering, Chinese Academy of Sciences. His research interests include image processing, underwater guidance navigation and control technology.